APPLICATION OF NONLINEAR AUTOREGRESSIVE NEURAL NETWORKS WITH EXOGENOUS INPUTS (NARX) IN SEISMIC FRAGILITY ANALYSIS OF BUILDINGS

By

IMRAN AHMED SHEIKH

Bachelor of Science in Civil Engineering

National University of Sciences and Technology

Islamabad, Pakistan

2015

Submitted to the Faculty of the
Graduate College of the
Oklahoma State University
in partial fulfillment of
the requirements for
the Degree of
MASTER OF SCIENCE
July, 2020

APPLICATION OF NONLINEAR AUTOREGRESSIVE NEURAL NETWORKS WITH EXOGENOUS INPUTS (NARX) IN SEISMIC FRAGILITY ANALYSIS OF BUILDINGS

Thesis Approved:

Dr. Mohamed Soliman

Thesis Adviser

Dr. Bruce W. Russell

Dr. Robert N. Emerson

ACKNOWLEDGEMENTS

I would like to thank Dr. Mohamed Soliman, my academic advisor, who constantly guided me throughout the course of my master degree. Without his supervision and support, this work would not have been possible. From the effective use of Powerpoint to MATLAB programming, I have learnt many things from him during my two years as his student.

I would like to thank my committee members, Dr. Bruce Russell and Dr. Robert Emerson, for reviewing my work and providing thoughtful and valuable feedback.

I would also like to thank Omid Khandel, PhD. candidate, who was always there as my mentor during my work. His experience and knowledge in the field of structural engineering helped me a lot in completing my thesis.

I am also thankful to Dr. Jennifer Hasse, who helped us in conducting structural health monitoring of a building. I would like to thank my friends and colleagues, Christopher Waite, Mohammad Firas Tamimi and Ligang Shen for their support.

Not but not least, I want to thank my parents who always encouraged me and provided moral support. Without their prayers and good wishes, this work would have not been possible.

Name: IMRAN AHMED SHEIKH

Date of Degree: JULY, 2020

Title of Study: APPLICATION OF NONLINEAR AUTOREGRESSIVE NEURAL NETWORKS WITH EXOGENOUS INPUTS (NARX) IN SEISMIC FRAGILITY ANALYSIS OF BUILDINGS

Major Field: CIVIL ENGINEERING

Abstract: Rapidly growing societal needs in urban areas are increasing the demand for tall buildings with complex structural systems. Many of these urban areas are located in zones characterized by high seismic activity. Quantifying the seismic resilience of these buildings require comprehensive fragility and risk assessment that integrates iterative nonlinear dynamic analyses to properly account for uncertainties. Under these circumstances, traditional finite element (FE) analysis may become impractical due to the high computational cost associated with fragility analysis. Soft-computing methods can be applied in the domain of nonlinear dynamic analysis to reduce the computational cost of seismic fragility analysis. Taking advantage of the computational efficiency of artificial neural networks, this study presents a framework that employs nonlinear autoregressive neural networks with exogenous input (NARX) in fragility analysis of multi-story buildings. The presented framework uses structural health monitoring data to calibrate a nonlinear FE structural model. The FE model is employed to generate the training dataset for NARX neural networks with acceleration and displacement time histories as input and output for the neural network, respectively. The trained NARX networks are then used to perform incremental dynamic analysis (IDA) for a suite of ground motions. Fragility analysis is next conducted based on the results of IDA obtained from the trained NARX network. The aforementioned framework is illustrated on a twelve-story reinforced concrete building located at Oklahoma State University, Stillwater campus. Results show that NARX networks have the potential to significantly improve the computational efficiency of fragility and reliability analysis of structures in seismically active regions.

TABLE OF CONTENTS

LIST OF FIGURES

Figure Page

Figure Page

CHAPTER I

INTRODUCTION AND LITERATURE REVIEW

The need to improve the resilience and sustainability of building infrastructure in active seismic zones has been increasing in recent years [1]. This demand requires structural engineers to design innovative and sometimes very complex structural systems to enhance the performance of new buildings under earthquake hazards. The dynamic response of these structures becomes highly intricate because of the significant contribution of higher modes [2]. These complexities add to the challenges of accurately predicting the behavior of these structures and the associated seismic demands [3]. In such situations, the most desired analysis procedure is the nonlinear dynamic analysis. Very often, especially during preliminary design phase, structural engineers are interested in quantifying a specific performance measure of the structure under different loading scenarios [2]. These performance measures include, for example, the maximum base shear or the maximum drift ratios under various earthquakes corresponding to different hazard levels [2]. In these situations, the iterative execution of full nonlinear dynamic analyses becomes necessary.

Over the past few years, several locations within the central Unites States experienced significant increase in earthquake activity due to induced seismicity [4]. Most of the structures in these areas are not designed to withstand this higher seismicity given the low natural earthquake hazard levels in these regions; accordingly, it is necessary to quantify the seismic risk of these vulnerable structures under updated seismic hazard scenarios. Performance-based earthquake

engineering (PBEE) [5] offers robust means for evaluating the seismic risk of structures with complex systems and irregular geometries. When used in conjunction with structural health monitoring (SHM), PBEE can provide a realistic prediction of the dynamic behavior of the investigated structure. A proper PBEE framework requires assessing the response at various hazard levels [6] and helps in quantifying the fragility of the structure. Fragility analysis [7], as an instrumental component of the risk assessment, can be conducted using incremental dynamic analysis (IDA) [7, 8] that analyzes the structure under a suite of ground motions with different intensity measures [9]. Hence, the process of developing the fragility curves for a given structure involves conducting numerous nonlinear analyses in order to properly incorporate underlying uncertainties [7].

Various finite element (FE) analysis software packages that are currently available can be used for conducting nonlinear dynamic analyses. In general, these packages can predict the seismic demand forces for complex structures with reasonable accuracy [10]. However, detailed nonlinear time history analysis (NLTHA) can be computationally very demanding and the computational cost has been reported to increase significantly for complex structural systems [11]. For instance, [3] analyzed a 55-story building using PERFORM 3D and reported a computational time of 30 hours. Accordingly, risk assessment that integrates traditional NLTHA may be deemed unfeasible. In these situations, it is necessary to develop more efficient and robust tools that can predict the nonlinear dynamic response of structures.

One approach to reduce this computational burden is to use surrogate models (i.e., metamodels) [12]. Soft computing methods, based on heuristic approaches, have been proposed to develop metamodels for various engineering problems. Artificial neural networks (ANNs), genetic algorithms, fuzzy logic, and decision tree analysis are among the popular methods in soft computing [3]. Owing to their computational efficiency and ability to predict accurate relationship between data points [13], ANNs have been widely used in solving structural engineering problems

[6] such as design optimization [14, 15], structural reliability analysis [16, 17], and damage detection and localization [18]. ANNs have also been used in the field of structural dynamics. For example, they have been implemented in [19] to predict displacement caused by dynamic loading on bridges. Additionally, [20] adopted multi-layer perceptron (MLP) architecture [21] to predict the dynamic response of various systems.

In the context of seismic response prediction of buildings, where nonlinear response at a certain time instant depends upon the previous state of the system (i.e., time series problems), regular neural networks such as MLP architectures suffer inefficiencies due to their simple architecture [10] and require numerous iterations for their training [22]. Therefore, research is still needed to develop approaches that can accurately predict the dynamic response of nonlinear structures using ANNs. Recently, [10] have implemented deep long short-term memory (LSTM) networks to predict the nonlinear seismic response of structures. However, training LSTM networks for datasets containing long range dependencies becomes difficult since LSTM networks may suffer from gradient vanishing problem [23]. This is a particular issue with the networks that utilize the gradient descent learning algorithms and have "hidden states" in their architecture [24] as is the case with LSTM networks. In [25], deep convolution neural networks have been applied for system identification and estimation of nonlinear structural dynamic response. However, as demonstrated in [25], deep convolution neural networks require a relatively large training dataset. The need for large training datasets negates the benefits sought after by using metamodels.

To address these limitations, nonlinear autoregressive neural networks with exogenous input (NARX) are used in this paper to predict the response of complex nonlinear dynamic systems. Recently, NARX neural networks have been used in various engineering problems involving modeling of nonlinear systems. Inundation levels during typhoons have been predicted in [26] using both open loop and closed loop NARX neural networks while [27] predicted energy consumption in buildings using NARX networks. These NARX networks not only use gradient

descent learning algorithms that are more efficient than other recurrent networks such as LSTM networks [24] but they also rely on tapped feedback delays which make them suitable for modeling systems with long range data dependencies [24]. This paper proposes a framework for seismic fragility analysis of buildings using NARX neural network. The presented approach integrates neural networks and nonlinear FE analysis to quantify the structural response during seismic excitations. SHM information collected during seismic events is used to calibrate key input parameters of the FE model. NARX neural networks are then trained using the results of nonlinear FE analyses of the structure. The trained NARX networks are used to obtain the critical peak ground accelerations and maximum interstory drift by means of incremental dynamic analysis. These quantities are next used to develop the seismic fragility curves of the investigated building. The framework is illustrated on an existing twelve-story reinforced concrete building in Stillwater, Oklahoma.

CHAPTER II

METHODOLOGY

Seismic Fragility Analysis

Fragility quantification is a crucial component in seismic risk assessment based on PBEE [7]. In addition to its role in risk assessment, fragility analysis is generally needed for retrofit design and post-disaster decision making and planning [28]. Seismic fragility can be defined as conditional probability of exceedance of a limit state function given a certain seismic intensity measure [3]. Mathematically, seismic fragility F_r can be expressed as [3]

$$F_r = P(LS > l \mid IM = m) \qquad (1)$$

where *LS* represents the limit state function, l being the limit of the function, *IM* represents the intensity measure, and *m* denotes a particular value of intensity measure.

Several approaches have been proposed for establishing the fragility curves of structural systems depending upon the processes used to capture the structural response. These approaches can be classified into three broad categories: (a) analytical approaches, which are based on investigating data obtained from structural analyses [29]; (b) empirical models, in which the statistical analysis of post-earthquake data is used to establish the exceedance measures [30]; and (c) heuristic approach based on the expert opinions [31].

To properly quantify the structural fragility, a model capable of representing the realistic nonlinear inelastic behavior of the system is required [3]. This can be achieved for newly designed

structures; however, for existing structures, developing an accurate numerical model may not be a straightforward task. For these structures, modeling difficulties may arise from the absence of detailed construction drawings, variations between the design and as-built characteristics, and unknown material properties. In addition, depending on the age of the structure, time-dependent deterioration (e.g., corrosion and concrete cracking) may have caused a shift in the structural properties that adds to the challenges in obtaining an accurate structural model. In this context, SHM plays a vital role in quantifying the realistic dynamic performance of the investigated structure [32]. During a seismic event, SHM can record the input excitation affecting the structure and the resulting response output. The structural performance parameters of interest are typically the accelerations and rotation, measured respectively by strong motion accelerometers and gyroscopes. By integrating SHM with system identification methods, the optimum values of key model parameters can be achieved resulting in a better representation of structural behavior [32]. Furthermore, SHM systems assist in detecting changes in the structural properties [33] and the occurrence of structural damage [34] along the service life of a structure.

Conducting nonlinear dynamic analysis can be achieved either by fast nonlinear analysis (FNA) or direct integration. FNA, also known as modal time history analysis, is based on modal analysis with a nonlinear force vector. Owing to its computational efficiency, it is widely used in the design community, but it has limited capabilities to incorporate the nonlinear attributes [35]. On other hand, the direct integration method is a step-by-step method which allows the inclusion of different nonlinear components within the analysis model [35]. This paper implements the direct integration method to allow modeling the nonlinear behavior using fibers and plastic hinges which cannot be properly considered using the FNA. Mathematically, the direct integration method involves solving the equation of motion

$$\boldsymbol{K}\, u(t) + \boldsymbol{C}\, u'(t) + \boldsymbol{M}\, u''(t) = F(t) \qquad (2)$$

in which ***K*** represents the stiffness matrix of the system, ***C*** represents damping matrix of the system, ***M*** is the mass matrix, *F(t)* is the force vector, and *u(t), u'(t), and u''(t)* are the displacement, velocity and acceleration vectors of the system, respectively. In general, FE solvers use numerical approaches to solve this system of equations such as Newmark's method [36] or Hilber-Hughes-Taylor method [37].

Incremental Dynamic Analysis (IDA), sometimes referred to as dynamic pushover analysis, is a parametric analysis technique that can be used to develop analytical fragility curves [8]. In the IDA, a suite of ground motion time histories, either real or simulated, are selected, scaled progressively, and applied to the nonlinear model of the structure until a specific limit state or failure criterion is achieved [9]. The incremental dynamic analysis results in the IDA curves which provide the relationship between the ground motion, as the intensity measure, and the engineering demand parameter of the structural response (e.g., maximum interstory drift). IDA not only provides a useful engineering insight on the behavior of a structure, but it provides deeper understanding of the structural response under different intensities of ground motion [9].

Analytical fragility curves can be established from the outcome of the dynamic analysis under multiple excitations using the Log-Normal (LN) cumulative distribution function (CDF). LN distribution model has been shown to provide accurate representation of seismic fragility [29, 38]. Due to the multiplicative reproducibility characteristic of the LN distribution, it has emerged as a powerful tool in the development of reliability and risk metrics [38]. Mathematically, a fragility function, based on LN CDF, is expressed as [39]

$$P(LS|IM) = \Phi\left(\frac{\ln(IM/\mu)}{\sigma}\right) \qquad (3)$$

where Φ represents the cumulative standard normal distribution, *IM* is the intensity measure, *LS* is the limit state, μ is median and σ is logarithmic standard deviation of the sample. However, as indicated earlier, conducting several full-scale dynamic analyses may not be computationally

feasible, especially when nonlinear behavior is incorporated in the model. Alternatively, the approach presented in this paper uses soft-computing tools to reduce this computational burden. Herein, a trained NARX neural network will be used to conduct the IDA for developing fragility curves of the investigated structure. A trained neural network can be used to conduct IDA for developing fragility curves.

NARX Neural Network

NARX is a nonlinear, dynamic model that relates two time series, an input/independent time series to an output/dependent time series [40]. It estimates the current value of a time series data with respect to past values of the same series and the current and past values of an exogenous/independent series. Mathematically, it can be represented as [24]

$$u(t) = G\big(u(t-1), u(t-2), \dots, u(t-k), v(t), v(t-1), v(t-2), \dots, v(t-k)\big) \qquad (4)$$

where u is dependent/output time series, v is independent/input or exogenous time series, k represents the number of feedback and/or input delays and G is nonlinear mapping function [41]. When this nonlinear function G is approximated using neural networks, the resulting system is known as NARX neural network [40]. A neural network is an algorithm intended to identify numerical patterns in data. A neural network consists of at least three layers; input, hidden and output layers. The input layer introduces input data to the neural network which is then fed to the hidden layer(s). The output layer is the last layer of a neural network which yields the output of the network [42].

Apart from these layers, there are two essential parameters of a neural network; activations functions and model parameters. An activation function accepts an input value and yields an output value by transforming the activation level of a neuron [43]. The model parameters are the weights and bias values associated with the connections between the neurons of a network. Mathematically, a neural network can be represented by a linear combination as [43]

$$y = f(w * x + b) \qquad (5)$$

where x represents the input parameters, y represents the output quantities, f denotes the activation function and w and b represents the weights and bias values, respectively. These weights and bias values are adjusted during the training phase of the neural network which results in the estimation of the mapping function. Hence training a neural network is establishing the optimum values of these weights and bias values. A network training function is used to update these model parameters by evaluating a cost function such that the difference between the predicted values by the network and the target values is minimum [44]. Mean squared error (MSE) is one of the commonly used cost functions [45]

$$MSE = \frac{1}{n}\sum_{i=1}^{n}(u_{network} - u_{actual})^2 \qquad (6)$$

where $u_{network}$ is the value predicted by neural network, u_{actual} is the target value, and n is the number of points in a given input. Figure 1 shows configuration of a typical neural network.

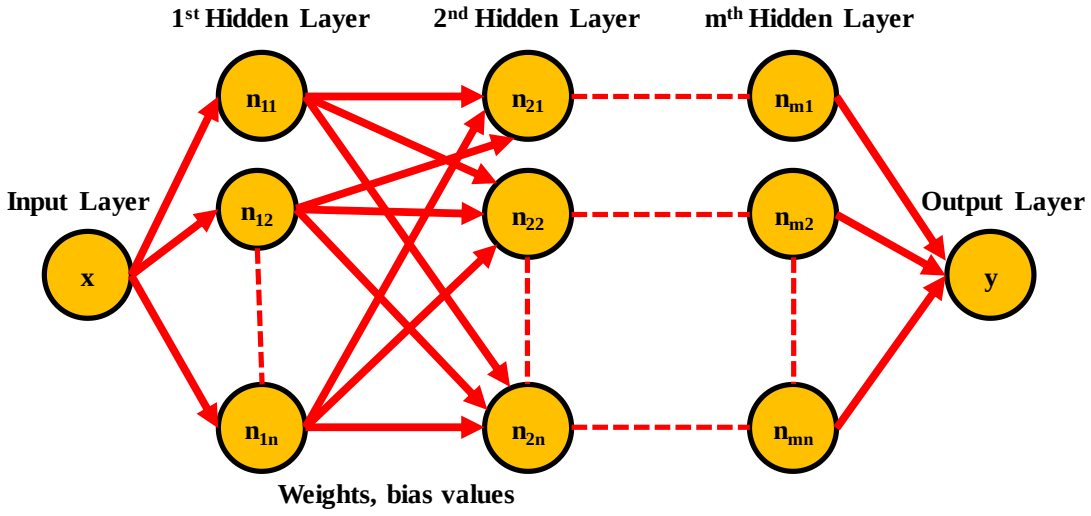

Figure 1. Typical configuration of a neural network

NARX is a type of neural networks that can be implemented in both feedforward and recurrent network configurations. A feedforward network consists of a series of layers where input layer and output layer sandwich the hidden layer(s) [46]. There are no closed loops in this network configuration, hence no feedback, and the data flows in one direction. However, in a recurrent neural network, there are closed loops which provide feedback in the form of output data to the input of neural network again [26]. NARX neural networks have been shown to be very efficient than ordinary neural networks; hence these networks are known to be equivalent to Turing machines [41]. A NARX neural network can be used in both architectures; open loop (or series-parallel) and closed loop (or parallel) [41] as shown in Figure 2. In open loop, both time series are given as input to the model, while in closed loop architecture, the NARX predicts the value of dependent series in a recurrent manner [26].

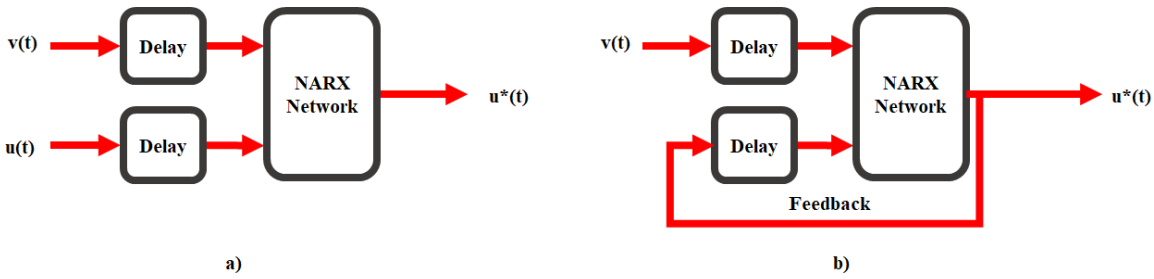

Figure 2. Configuration of NARX neural network: a) open loop, b) closed loop

In this paper, NARX networks are used within an integrated framework for quantifying the seismic fragility of multistory buildings. The layout of the framework is shown in Figure 3. The framework starts with constructing the finite element model of the investigated structure. In this phase, a nonlinear structural model is required to properly represent the realistic behavior of the structure during seismic events. SHM data is integrated to calibrate the structural model; however, the framework can also be applied if no SHM data is available. A suite of ground motion records is

selected based on magnitude and source to site distance. The calibrated FE model is then used to conduct nonlinear dynamic analyses to generate the training and testing datasets for NARX neural networks. The dataset is next used to train and validate the NARX neural networks. Once trained, the NARX networks are then used to conduct the IDA considering PGA as the intensity measure and maximum IDR as the engineering demand parameter. Seismic fragility curves are then developed based on the generated IDA curves.

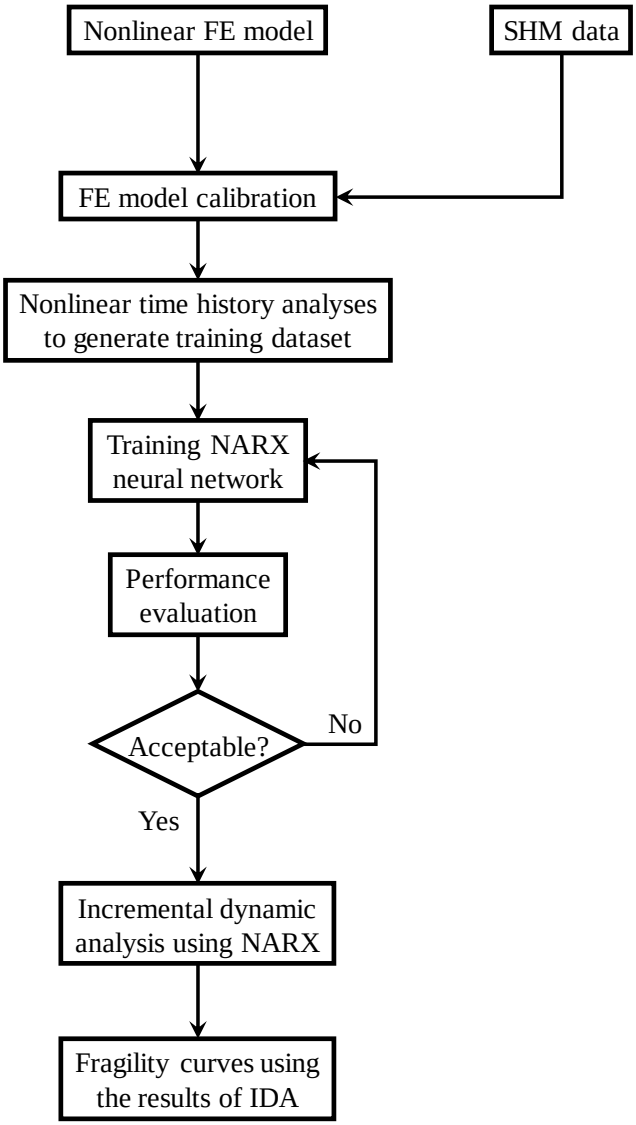

Figure 3. Layout of the proposed framework for conducting fragility analysis using NARX neural networks

CHAPTER III

ILLUSTRATIVE EXAMPLE

The presented framework for fragility analysis using NARX neural networks is illustrated on a twelve-story reinforced concrete building located on the campus of Oklahoma State University, Stillwater. The selected building, Kerr hall, is a residential building constructed in the 1970. The building is 187.5 ft long and 55.34 ft wide with a total height of 122.3 ft. The height of first story is 12.3 ft while rest of the stories are 10 ft high. The lateral load resisting system consists of moment frames and shear walls while the gravity load system consists of reinforced concrete slabs and gravity columns. The building has two staircases and two shear wall cores that house the elevators. Figure 4 shows the plan view of the investigated building. Given the increase in the seismic activity in the region, the building was instrumented to assess its acceleration response, rotations and displacements during seismic events. A GPS antenna, shown in Figure 5, was installed on the roof level of the building to measure the real-time displacements during an earthquake. The difference between the GPS positions before and after an earthquake can provide the residual deformations. Two triaxial strong motion accelerometers, one at ground level and one at roof, were mounted to record the ground acceleration and building response during an earthquake. Similarly, two triaxial gyroscopes were installed to capture the rotational behavior of the building during seismic events. Figure 6 shows the installed accelerometer and gyroscope:

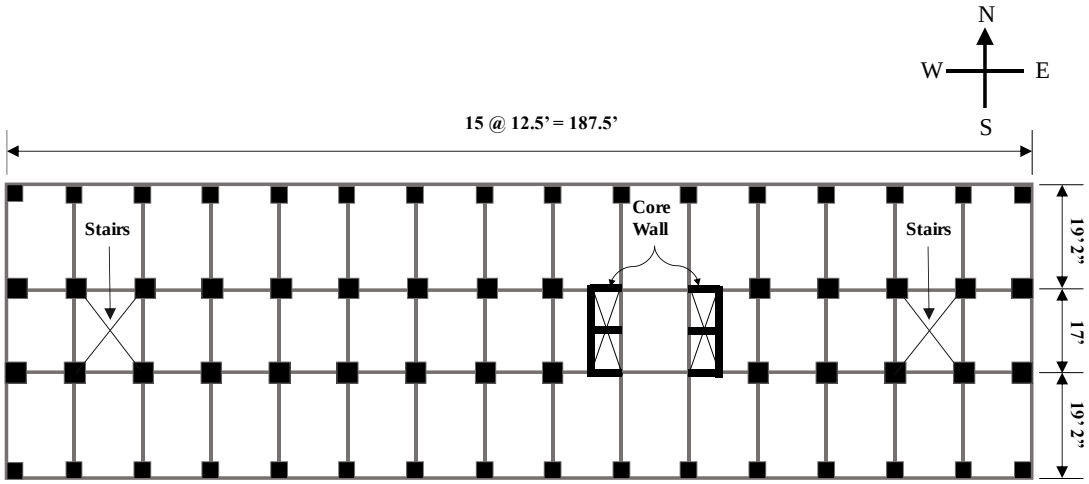

Figure 4. Plan of the building

Figure 5. GPS antenna mounted on the building

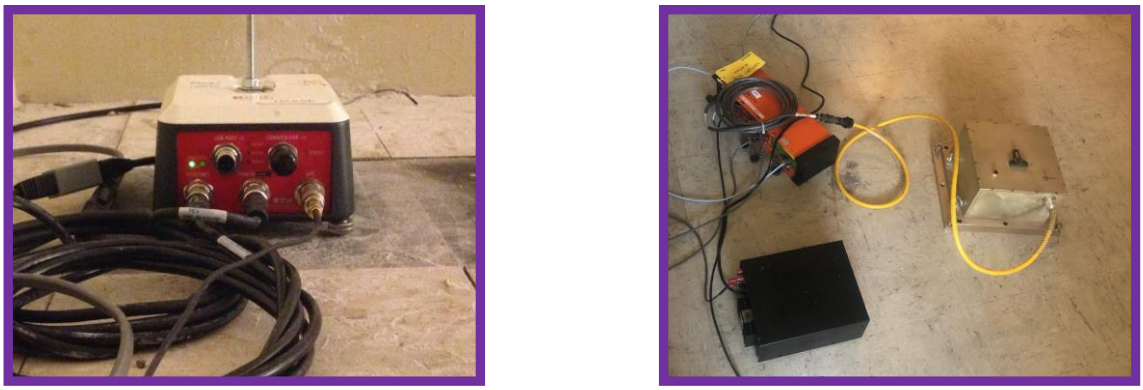

Accelerometer **Gyroscope**

Figure 6. Accelerometer and gyroscope installed in the building

On April 07, 2018, an earthquake of magnitude 4.6 struck northern Oklahoma. The epicenter was located at approximately 29 miles from the investigated building at a depth of 6.25 miles. At the time of the earthquake, only the triaxial accelerometers were fully functional. Accordingly, only the acceleration time histories recorded during this earthquake will be used herein to calibrate the finite element model of the building.

Finite Element Modeling

A three-dimensional finite element model of the building, as shown in Figure 7, is created in CSi SAP2000 environment [35] based on the as-built structural drawings provided by university administration.

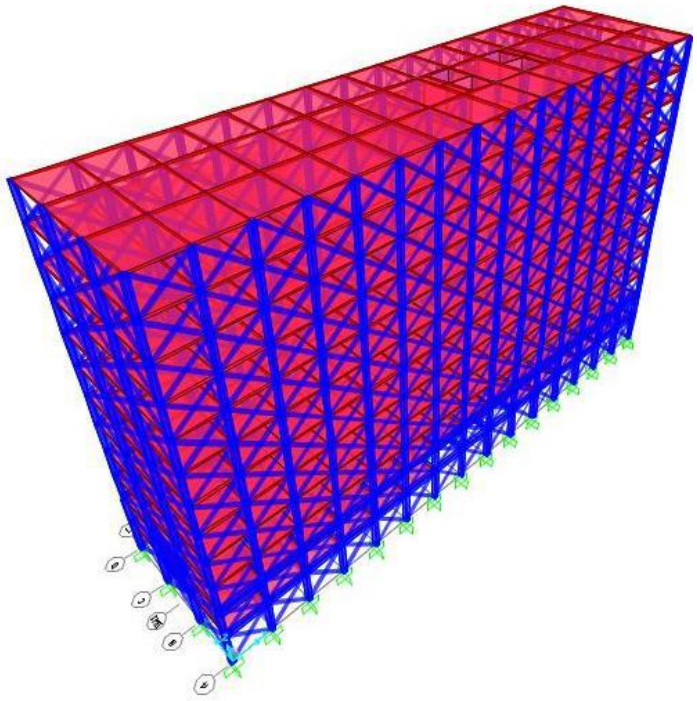

Figure 7. Finite element model of the building in CSi SAP2000

Nonlinearity in the model is introduced at both the material and geometric levels. Reinforced concrete is modeled using Mander's concrete model [47] as an isotropic material with cylinder compressive strength of 5,000 psi for columns and shear walls, and 4,000 psi for all other members. Figure 8 shows the stress-strain curve for 5,000 psi concrete used in this analysis. A parametric stress-strain model which takes into account the strain hardening behavior [35] is used for the steel reinforcement. The stress-strain profile for the adopted parametric model is given as

$$\sigma = \begin{cases} E\varepsilon & for\ \varepsilon < \varepsilon_y \\ \sigma_y & for\ \varepsilon_y < \varepsilon < \varepsilon_{sh} \\ \sigma_y + (\sigma_u - \sigma_y)\sqrt{\dfrac{\varepsilon - \varepsilon_{sh}}{\varepsilon_u - \varepsilon_{sh}}} & for\ \varepsilon > \varepsilon_{sh} \end{cases} \quad (7)$$

in which σ is the rebar stress, E is the modulus of elasticity, ε is the rebar strain, σ_y represents the yield stress, σ_u is the ultimate stress, ε_{sh} is the strain at the onset of strain hardening, and ε_u is the ultimate strain. Figure 9 shows the stress-strain profile for the steel reinforcement with yield strength of 50,000 psi used in this model.

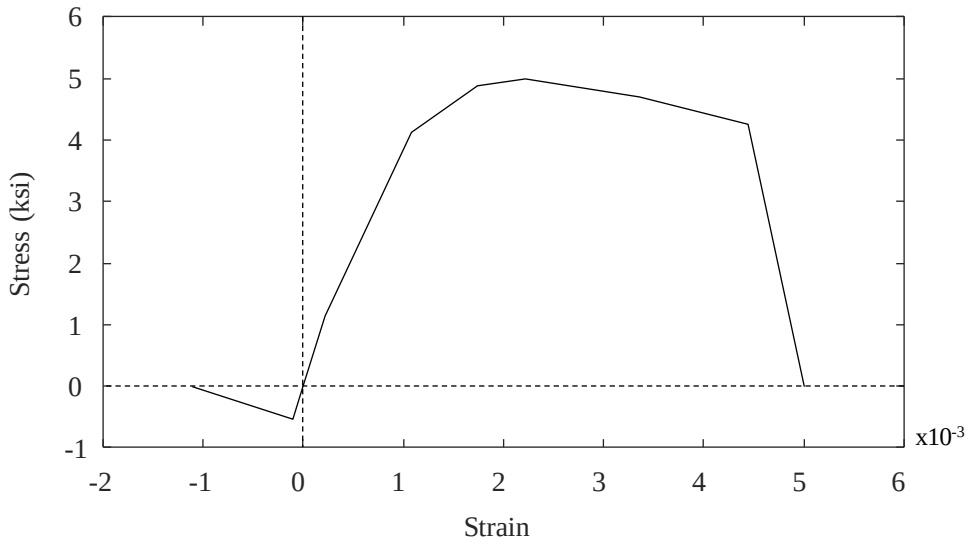

Figure 8. Stress-strain curve of 5,000 psi concrete using Mander's model

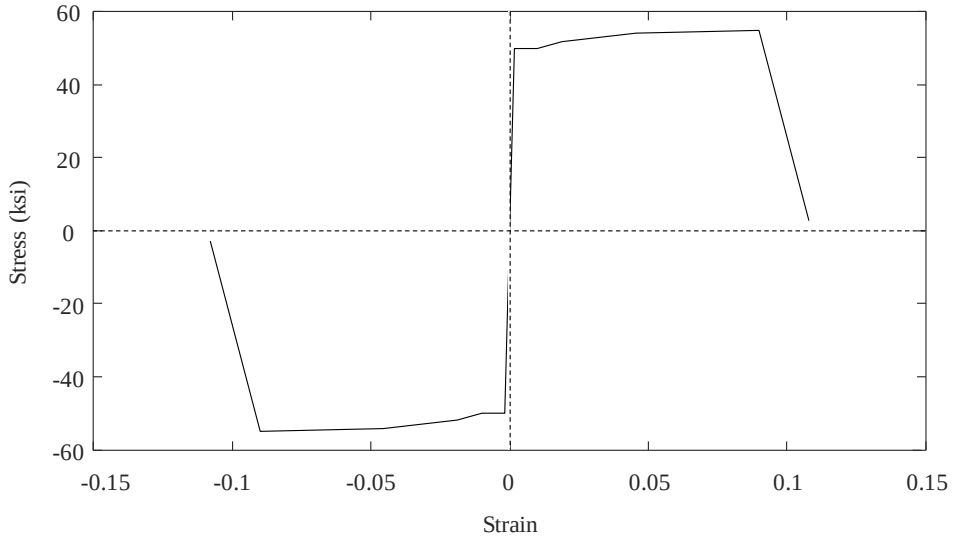

Figure 9. Parametric stress-strain relationship for steel reinforcement with yield stress of 50 ksi

Fiber modeling is adopted to include the inelastic sectional behavior of columns. This technique allows the inclusion of plasticity distribution along the member and across its cross-section [48, 49]. In the fiber modelling approach, the cross-section of the column is divided into small axial fibers. Depending upon the material, whether steel or concrete, each fiber is assigned its own nonlinear stress-strain curve. This process allows capturing the axial force and moment interaction in the elements, as well as the effects of cracking and yielding across and along the member [50]. Integrating the resultant behavior on the cross-section level along the length using the aforementioned material constitutive laws provides the required force-deformation relationships. This approach is not only suitable for nonlinear inelastic response under dynamic loadings but also provides reliable and efficient solution [6]. Figure 10 shows a schematic representation of fiber modeling approach:

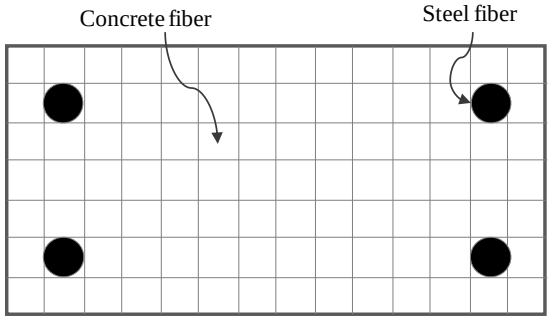

Figure 10. Typical cross-section in fiber modeling approach

Plastic hinges are assigned to the ends of the beams to model the nonlinear frame behavior as lumped plasticity. Plastic hinge modeling has been shown to properly represent the building behavior near collapse loading conditions and also allow capturing the concrete crushing and rebar buckling behavior in the model [5]. Simulating the nonlinear behavior of plastic hinges was achieved by defining a backbone curve as opposed to fiber modeling where each fiber is assigned a full nonlinear stress-strain curve. The backbone curve parameters (i.e. plastic rotation angle and residual strength ratio) are selected herein based on FEMA 356 [51]. A plastic hinge backbone

curve is shown in Figure 11 where ‘a’, ‘b’, and ‘c’ are parameters that depend on the material properties, cross-sectional dimensions, and reinforcement ratio [51].

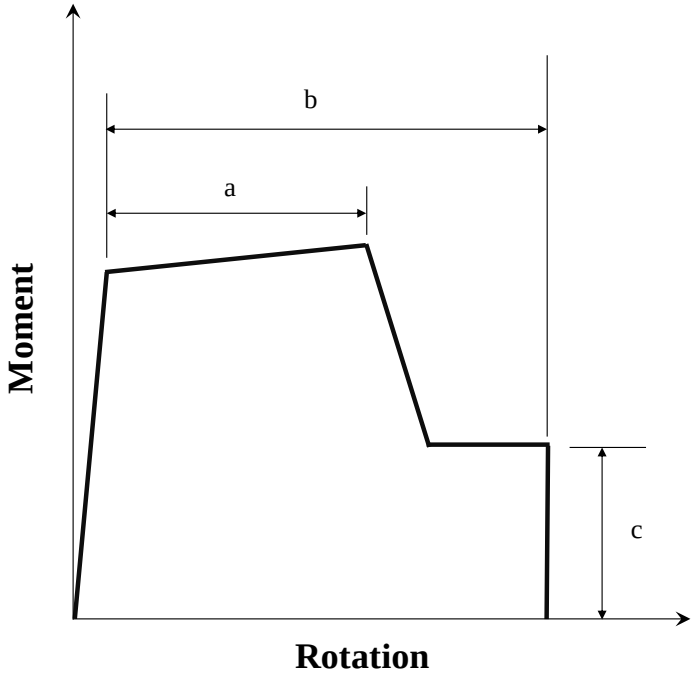

Figure 11. Backbone curve for plastic hinge using FEMA 356 [51]

The hysteretic behavior is incorporated in this example using Takeda’s stiffness degrading model [52]. This model was shown to represent the realistic behavior of reinforced concrete systems under dynamic loading [52]. It takes into account the change in stiffness associated with flexural cracking and yielding of reinforcement in addition to incorporating the strain-hardening effects [53]. In this model, the unloading curve follows the elastic portion of the backbone curve and the reloading curve follows a secant line. If the applied load exceeds the yield load, the unloading curve follows an exponential function [52]. However, this exponential unloading behavior is considered linear due to software limitation. Maximum deformation point for previous cycle becomes the target point for the secant line in next cycle. As a result, the hysteresis loop continues to reflect the reduction in energy dissipation with increased deformation levels. Since hysteretic damping is already

considered within the hysteresis behavior, Rayleigh damping of 4% is used to account for viscous damping as opposed to traditionally adopted 5% [50]. Second-order nonlinear behavior is also incorporated explicitly in the model.

Being a residential hall, the building consists of a large number of infill walls that have a significant influence on the stiffness of the structure. The stiffness contribution of infill walls is included in the model using equivalent diagonal compression-only struts following FEMA 356 recommendations [51]. The strut thickness is chosen equal to the thickness of the walls while the width of the strut *a* is calculated as [51]

$$a = 0.175\ (\lambda_1 h_{col})^{-0.4} r_{inf} \qquad (8)$$

in which

$$\lambda_1 = \left[\frac{E_{me} t_{inf} \sin 2\theta}{4 E_{fe} I_{col} h_{inf}}\right]^{\frac{1}{4}} \qquad (9)$$

where t_{inf} is the thickness of infill wall and strut, L_{inf} is the length of infill wall, r_{inf} represents the diagonal length of infill wall, I_{col} is the second moment of area of column, E_{me} is the expected elastic modulus of infill wall, E_{fe} is expected elastic modulus of frame, h_{inf} is the height of infill wall, h_{col} is the height of column, and θ represents the angle whose tangent is the infill height-to-length ratio.

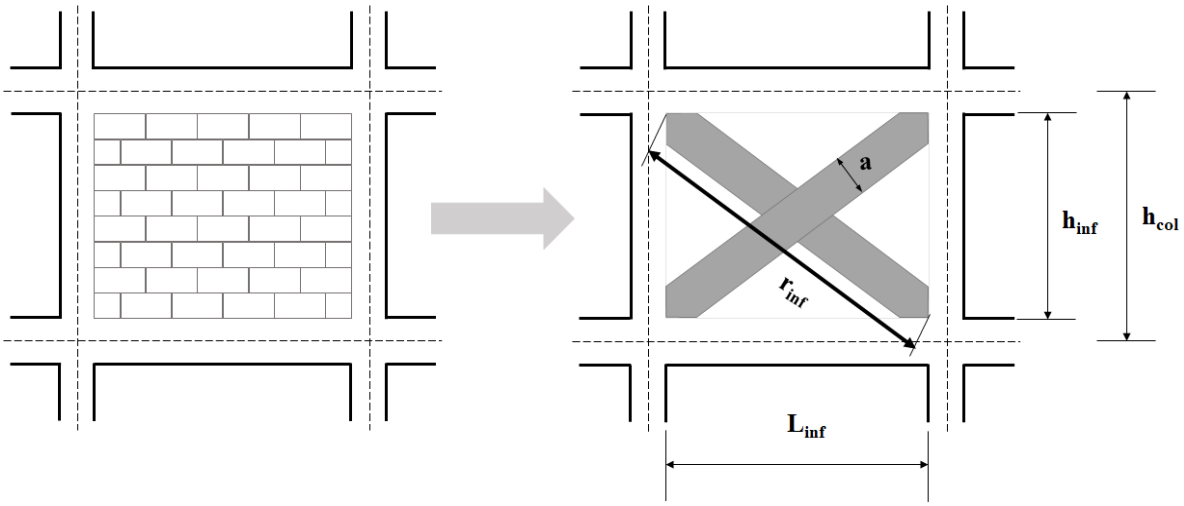

Figure 12. Equivalent diagonal compression strut model using FEMA 356

The behavior of all floor slabs is assumed elastic and they are modeled as thin shell elements where transverse shear deformations are neglected. Rigid diaphragms are assigned to each story level to model the in-plane stiffness.

FE Model Calibration

To improve the ability of the FE model to represent the analyzed structure, SHM information is used to calibrate the structural model. The ground acceleration recorded during the April 07, 2018 earthquake is applied to the finite element model and the corresponding recorded roof acceleration is compared to the time history resulting from the FE model under the same excitation.

Bending stiffness values of columns along both axes are chosen as calibration parameters. Optimum values of these parameters are determined such that the difference between the modal frequencies obtained from SHM data analysis and the finite element model is minimized. For this optimization, the objective function is defined as

$$g(X) = \sum_{i=1}^{n} W_i \cdot \left(\frac{f_{a,i}(X) - f_{m,i}(X)}{f_{m,i}(X)} \right)^2 \qquad (10)$$

where $g(X)$ is the objective function, $f_{a,i}(X)$ is the computed natural frequency of mode i using finite element analysis, $f_{m,i}(X)$ is the measured natural frequency of mode i using SHM data analysis, W_i is the weighting factor of mode i, n is the number of considered vibration modes, and X is the vector of calibration parameters. This optimization problem is solved using sequential quadratic programming algorithm to establish the optimum values of the column stiffness. The first three natural modes of the building, which cover almost 90% of the modal mass participation, are considered for model calibration.

Figures 13 and 14 show the roof-to-base power spectral density (PSD) ratio for the SHM recorded response and calibrated FE model in both directions. As shown, the FE model is capable of representing the structural behavior. The power spectral ratio of FE model and actual structure are close in both low and high frequency ranges.

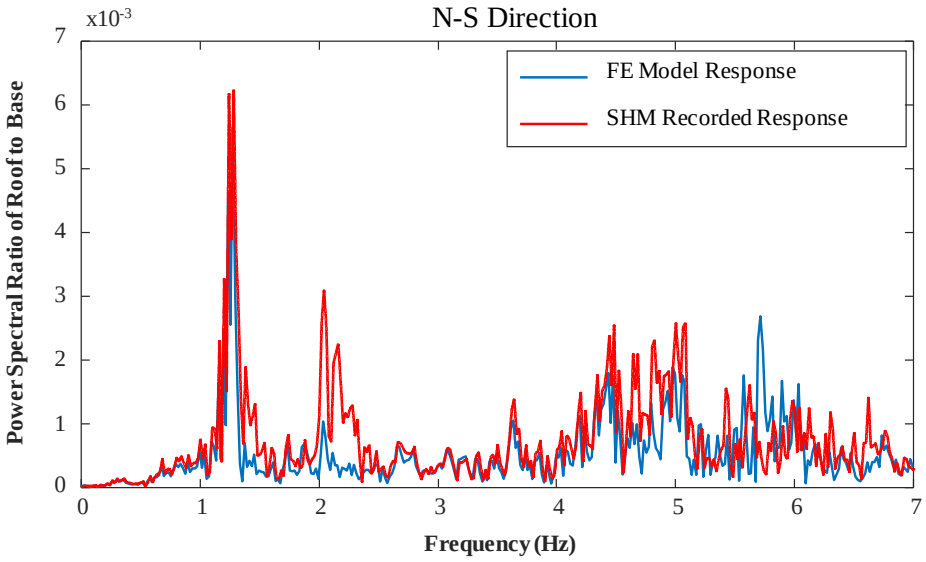

Figure 13. Comparison of PSD ratio (N-S direction)

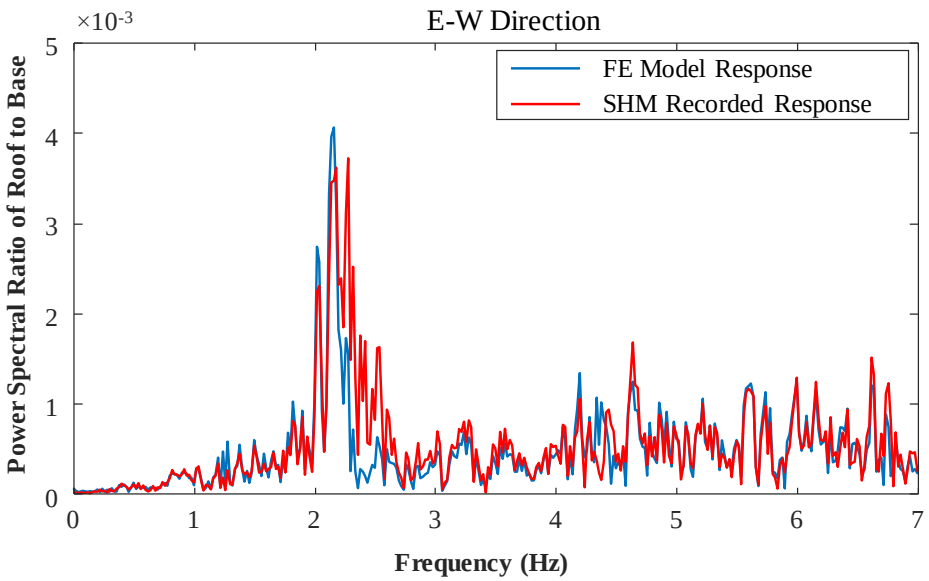

Figure 14. Comparison of PSD ratio (E-W direction)

Figure 15 shows the probability plot of the frequencies at which peaks occur in the roof-to-base PSD ratio plots obtained from SHM data and the FE model. As shown, the FE model reports the peak values to occur at almost the same frequencies at which the SHM data shows peaks especially in lower frequencies that have higher contribution to the system response.

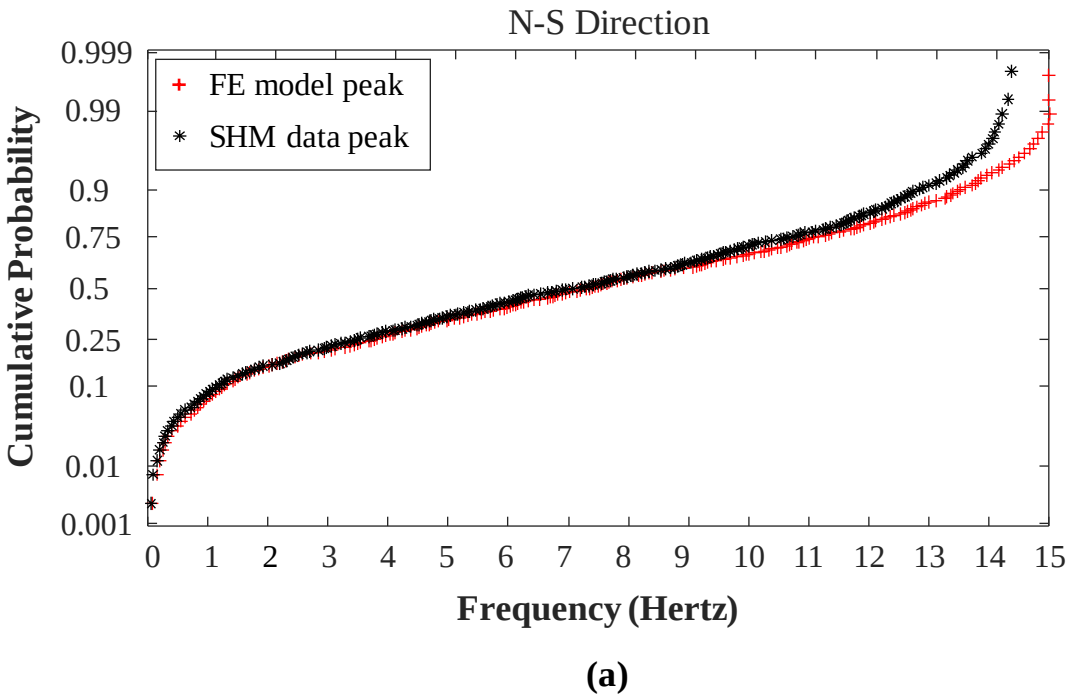

(a)

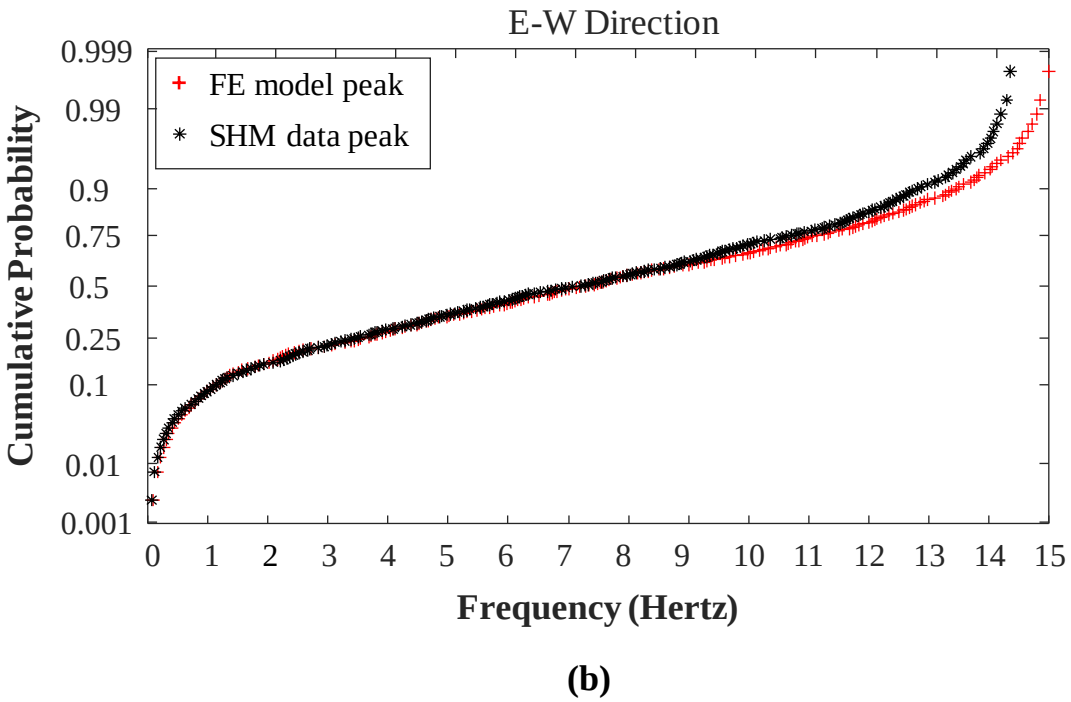

(b)

Figure 15. Probability plot comparing occurrence of peaks in PSD ratio for SHM and FE model, (a) N-S direction; (b) E-W direction

Figure 16 shows the acceleration response recorded using SHM and FE model for the April 07, 2018 earthquake. As it can be seen from this figure, the FE model is capable of predicting the dynamic response of the building under seismic excitations.

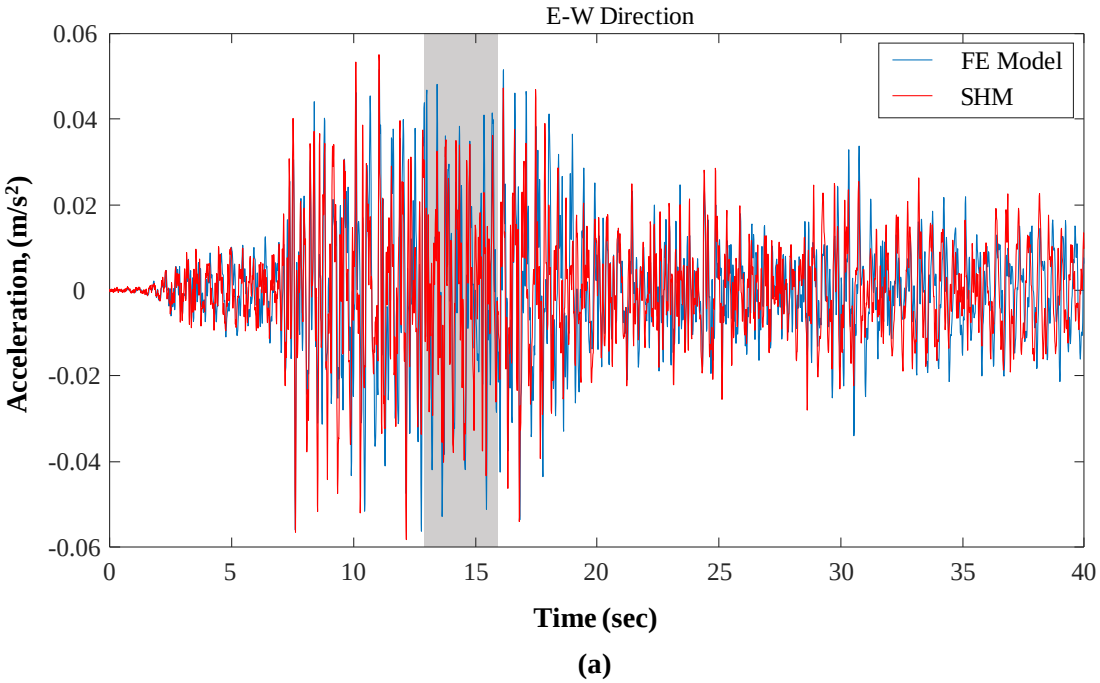

(a)

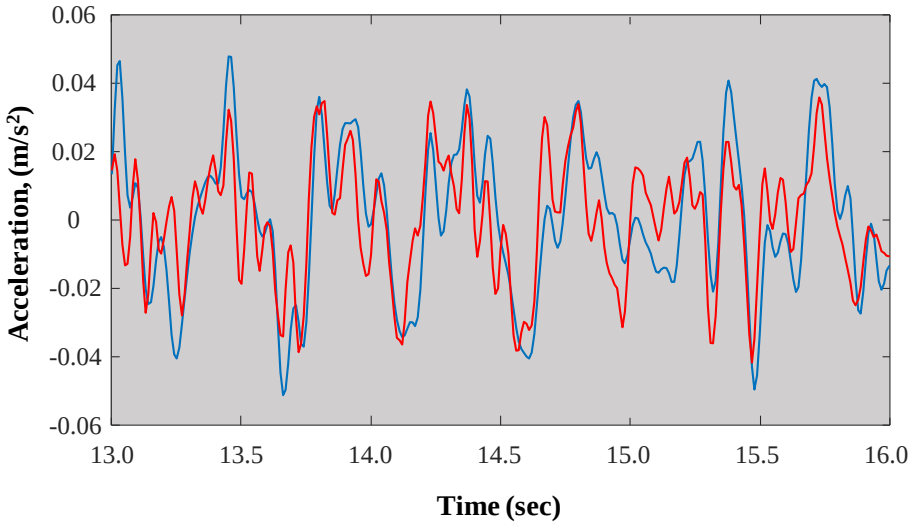

(b)

Figure 16. (a) Acceleration response comparison of FE model with SHM; (b) From 13 seconds to 16 seconds

Earthquake Selection

Ground motion records of real earthquakes are downloaded from Next Generation Attenuation (NGA-West2) database created by the Pacific Earthquake Engineering Research (PEER) center [54]. The selected earthquake records have magnitude range of 4.0 – 7.5 and Joyner-Boore distance R_{JB} [54] of less than 100 km. The selected acceleration time histories are then used in finite element analysis to generate the training dataset for NARX neural networks.

Neural Network Training and Testing

The NARX neural network is implemented using the neural network toolbox in MATLAB [46]. In this paper, tan-sigmoid transfer function in hidden layer and linear transfer function in the output layer is used. Acceleration time histories are chosen as input and FE analysis results (i.e., displacement time histories) are chosen as target values. Bayesian Regularization [56] is adopted as the training function to determine the optimum combination of bias values and weights that minimizes the neural network prediction errors.

A total of 10 ground motion records are used to train the model. NLTHA is conducted for each selected earthquake using step-by-step direct integration in CSi SAP2000 [35]. The selected ground motions and their corresponding displacement time histories are then used to train the NARX neural networks. For training the network, open loop NARX neural network is used as both input and output data are available during the training phase. The configuration of a neural network is one of the most important aspect in determining its performance. As no significant literature is available for NARX network configuration in nonlinear seismic response prediction applications, a trial network configuration with one hidden layer of 5 neurons and input and feedback delay of 10 is selected. With this configuration, it is observed that the network is unable to accurately predict the dynamic response. After various systematic trials, a network configuration of 1 hidden layer with 10 neurons is selected. Moreover, the number of input and feedback delays are selected as

multiples of fundamental time period of the building. Delay of 80 values (which is approximately half of the fundamental time period, T=0.77 sec, where 0.005 sec is the time step) for both input and feedback layers is used. With this configuration, accurate network performance is observed.

A separate network is trained to predict the response time history of each story. Training data are scaled to range between -1, +1 in order to improve the training efficiency of the model [10]. The weights and bias values are adjusted iteratively during the training using back-propagation algorithm such that the error between the predicted network values and target values reach a minimum. Mean squared error (MSE), as shown in Equation (6), is taken as the training performance indicator [23]. Figure 17 shows the variation of MSE with respect to the number of neurons. It can be seen from the figure that adding more number of neurons after 10 does not decrease the MSE appreciably; hence, 10 neurons are used for training purposes.

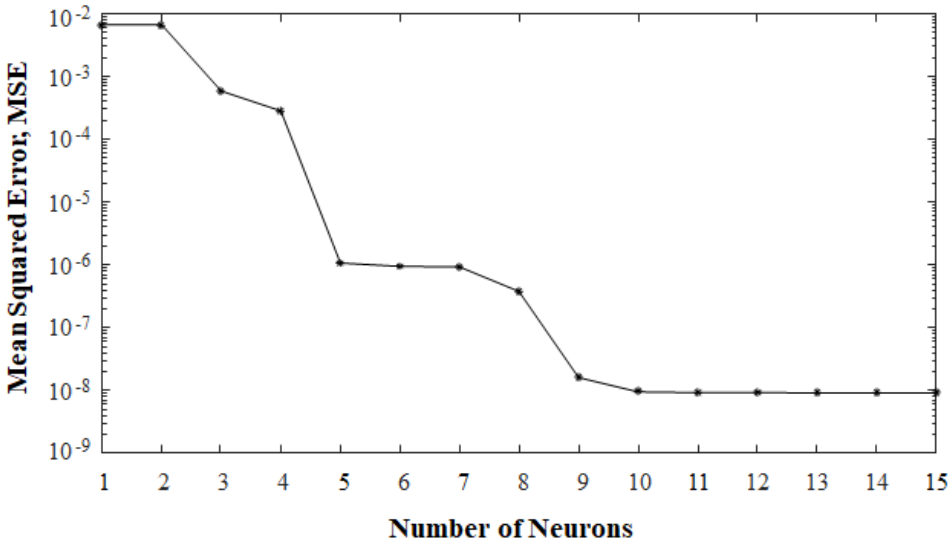

Figure 17. Variation of Mean Squared Error (MSE) with number of neurons

Once the networks are trained, they are converted into closed loop configuration to assess their performance accuracy using another set of earthquakes that are not used in training phase. Figures 18 and 19 show the predicted response of the trained neural network, under an earthquake, for first

and twelfth stories, respectively. As shown, the NARX neural network is capable of predicting the displacement time history with appreciable accuracy. Figure 20 compares the probability plot of displacement amplitudes using FE analysis with NARX predictions. As shown, reasonable prediction accuracy can be observed.

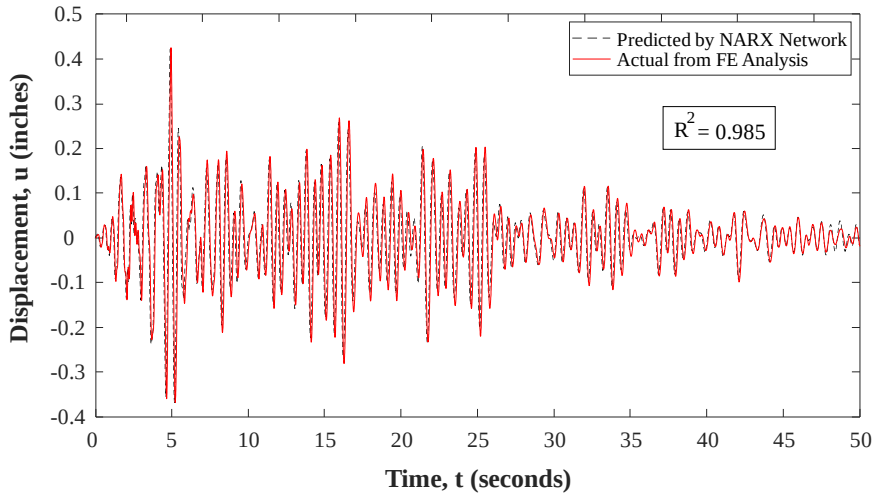

Figure 18. Comparison of displacement response prediction of NARX network with FE analysis (First story)

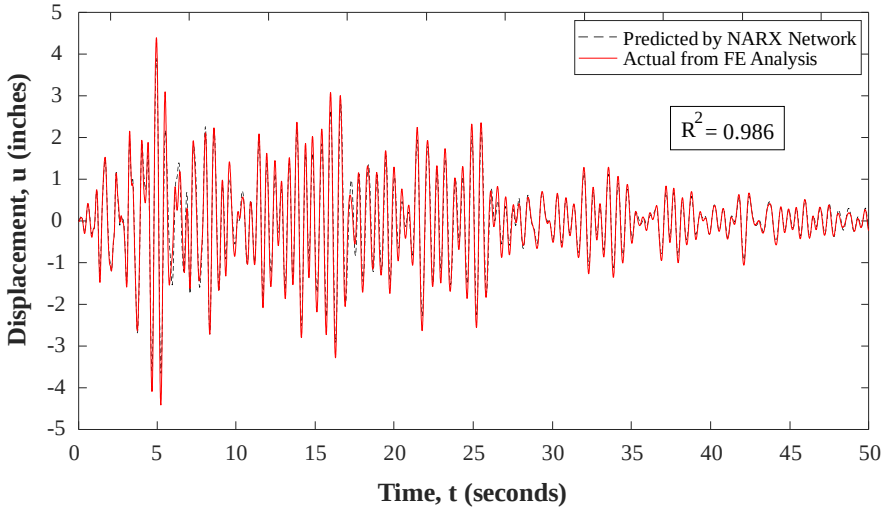

Figure 19. Comparison of displacement response prediction of NARX network with FE analysis (Twelfth story)

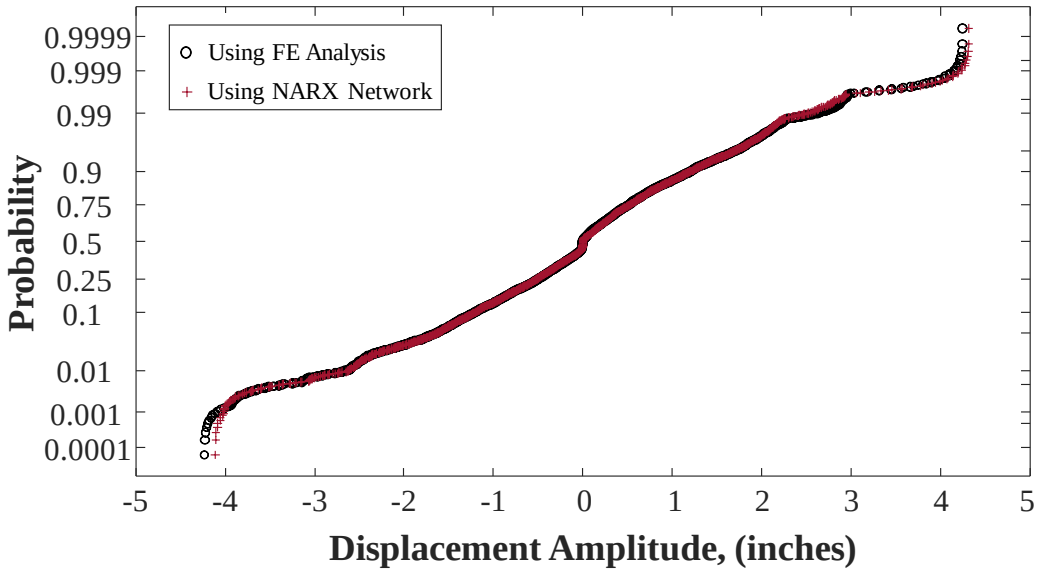

Figure 20. Probability plot of displacement values obtained from FE analysis vs. predicted by NARX

Incremental Dynamic Analysis

The trained networks in closed loop configuration are used to conduct the incremental dynamic analysis (IDA). Peak Ground Acceleration (PGA) is taken as intensity measure (IM) and the interstory drift ratio (IDR) is chosen as engineering demand parameter (EDP). Fifteen ground motions are selected and scaled to cover various levels of peak ground acceleration (PGA), starting from 0.05g with 0.05g increments until failure. Failure is assumed when the maximum IDR reaches or exceeds 3%, which is more than the 2.5% collapse prevention limit [8]. Figure 21 shows the profile of maximum IDR with respect to story level and the median maximum IDR with respect to story level. It can be seen from this figure that for a given intensity of a ground motion, 6^{th} and 7^{th} story experience relatively higher drifts than others.

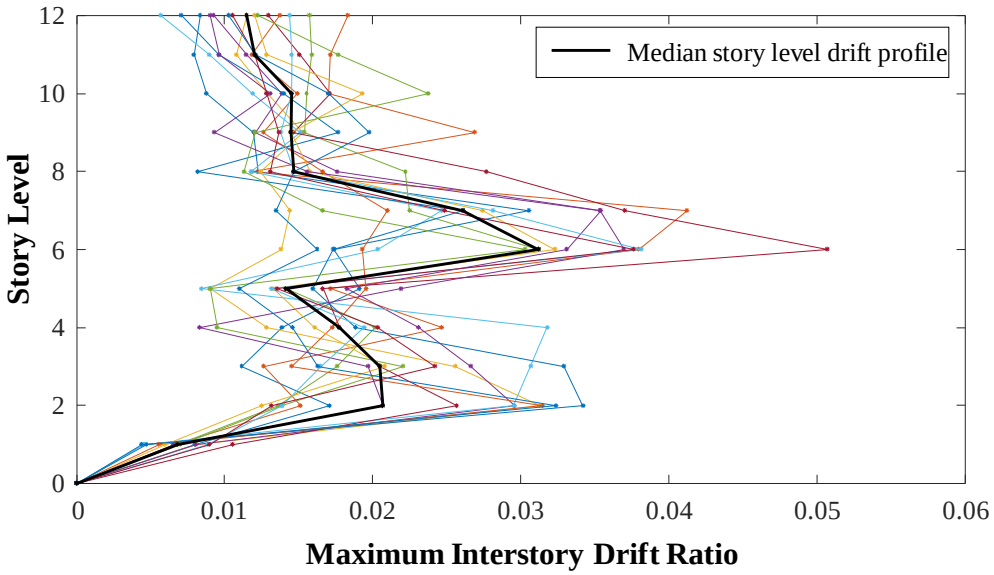

Figure 21. Maximum interstory drift ratio with respect to story level at collapse PGAs

Figure 22 shows the results of IDA for 15 earthquakes conducted using the trained NARX neural networks in terms of PGA versus maximum IDR along with median maximum IDR. As shown, the maximum IDR increases linearly till PGA of almost 0.6g, depicting linear behavior of the building. After 0.6g, softening occurs, signaling the onset of nonlinear behavior.

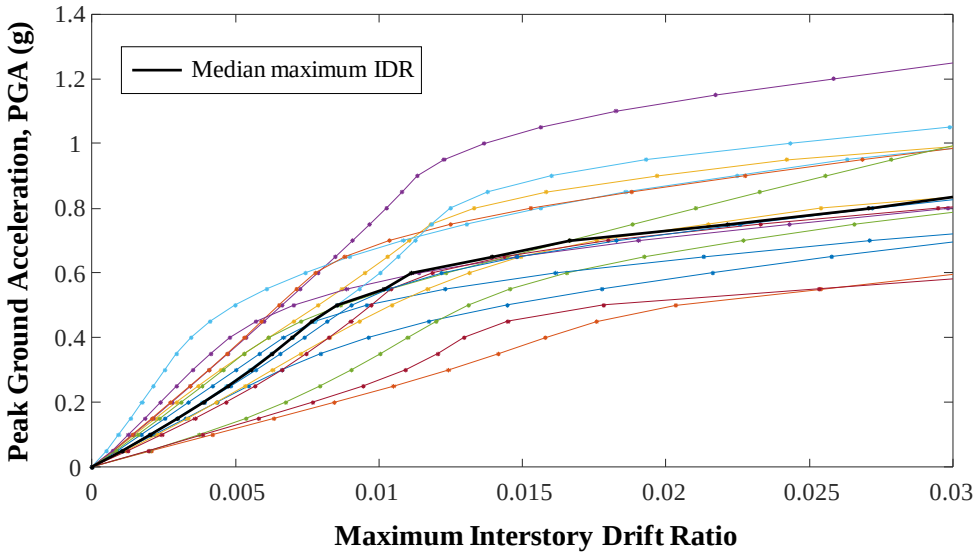

Figure 22. IDA analysis results conducted using NARX networks

NARX networks conducted the IDA analysis, shown in Figure 22, in approximately five minutes. On the other hand, conducting nonlinear dynamic analysis for one earthquake using SAP2000 required approximately four hours. This translates to more than 45 days to complete such analysis using traditional nonlinear FE analysis. The analysis has been conducted on a desktop computer with Intel(R) Core (TM) i7-7700 CPU at 3.60 GHz and 16 GB of RAM.

Seismic Fragility Analysis

After conducting the IDA, the fragility curves are developed using Equation (3). Figure 23 shows the fragility curve based on lognormal cumulative distribution. It can be seen from the figure that the probability of failure (i.e. probability of exceedance of 3% drift ratio limit state) is 50% for PGA value of 0.85g and almost 100% at 1.3g.

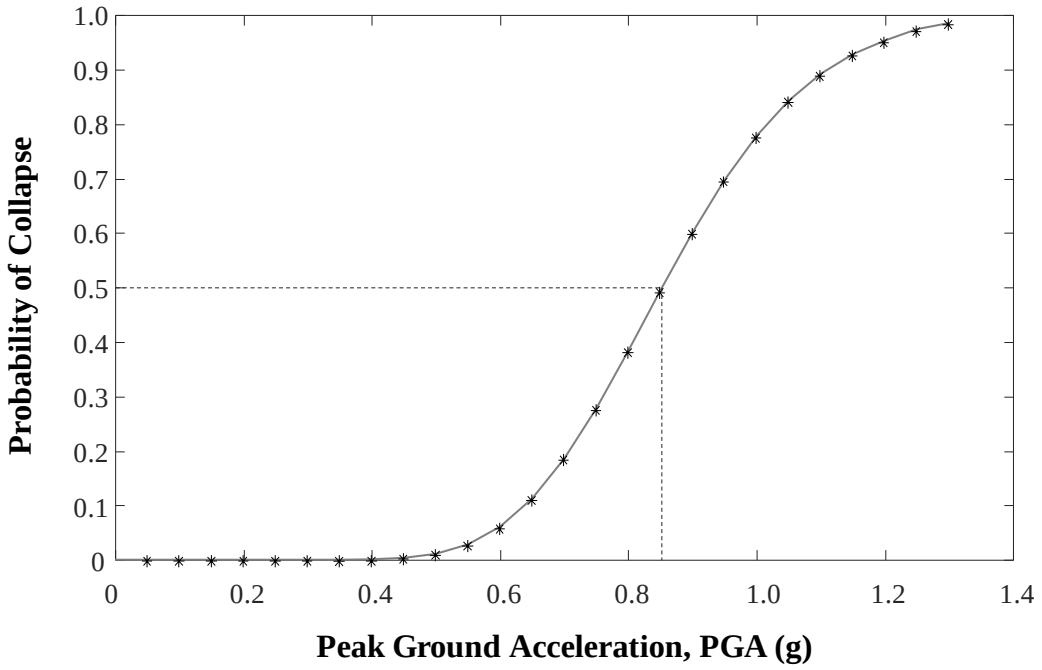

Figure 23. Seismic fragility curve

CHAPTER IV

CONCLUSIONS AND FUTURE WORK

Conclusions

This paper presented a framework for conducting seismic fragility analysis of multi-story buildings using nonlinear autoregressive exogenous (NARX) input neural network. The study integrates structural health monitoring data with finite element (FE) analysis to calibrate a structural model. A relatively small number of analysis results conducted on the calibrated FE model are used to train and test the NARX networks. The trained networks are then used to conduct incremental dynamic analysis (IDA). The results of IDA are then used to construct the seismic fragility curves of the building. The presented framework was illustrated on a twelve-story reinforced concrete building. The following conclusion can be drawn:

- NARX neural networks are capable of predicting the nonlinear dynamic response of structural systems subjected to seismic excitations. However, care should be taken in generating the network training dataset to encompass the range of earthquakes required for the seismic fragility analysis.
- The defined feedback delay in the NARX network has a significant effect on the prediction accuracy. It was found that a delay of approximately 50% of the fundamental time period of the structure, both in input and feedback layers, yields optimum training of the NARX network. Lower feedback delay resulted in loss of accuracy results while larger delay required significantly longer training time without considerable gains in prediction

accuracy.

- IDA is an important tool in assessing the seismic behavior of structures. It provides the relationship between the seismic intensity and the corresponding structural response parameter. The IDA curves can be efficiently generated using the proposed framework for a given response parameter. Multiple response parameters can be included in the analysis; however, training time will be affected by the number of required response parameters.
- SHM plays an important role in performance assessment of existing structures. It provides system input and output signals that can be used to quantify the structural performance and calibrate the structural model.
- The proposed framework can efficiently construct the seismic fragility curves of multistory buildings. Integrating the FE analysis to generate the network training and testing data then using the neural network to construct the fragility curves led to a significant reduction in the computational time of the analysis.

Suggestions for Future Research

Having shown promising results in dynamic response prediction of buildings, the following potential research areas are suggested:

- Future studies are needed to further optimize the NARX network in the seismic response prediction of structures by identifying more advanced and robust training algorithms.
- The use of NARX neural network can be extended to include other types of structures such as bridges.

REFERENCES

[1] Sarkisian, M., Mathias, N., Garai, R. and Horiuchi, C. (2017). "Improving seismic resilience using structural systems with friction-base fuses." *In the Proceedings of the AEI Conference,* Oklahoma City, Oklahoma.

[2] Rajbhandari, A. M., Anwar, N., and Najam, F. (2017). "The use of artificial neural networks (ANN) for preliminary design of high-rise buildings." *In the Proceedings of 6th ECCOMAS Thematic Conference on Computational Methods in Structural Dynamics and Earthquake Engineering,* Rhodes Island, Greece.

[3] Zain, M., Anwar, N., Najam, F. A., and Mehmood, T. (2017). "Seismic fragility assessment of reinforced concrete high-rise buildings using the uncoupled modal response history analysis (UMRHA)." *In the Proceedings of International Conference on Earthquake Engineering and Structural Dynamics,* Reykjavik, Iceland.

[4] Ellsworth, W. L. (2013). "Injection-induced earthquakes." *Science,* 341(6142), 1225942.

[5] Shokrabadi, M., Banazadeh, M., Shokrabadi, M., and Mellati, A. (2015). "Assessment of seismic risks in code conforming reinforced concrete frames." *Engineering Structures,* 98, 14-28.

[6] Lagaros, N. D., and Papadrakakis, M. (2012). "Neural network based prediction schemes of the non-linear seismic response of 3D buildings." *Advances in Engineering Software,* 44, 92-115.

[7] Kiani, J., Camp, C., and Pezeshk, S. (2019). "On the application of machine learning techniques to derive seismic fragility curves." *Computers and Structures,* 218, 108-122.

[8] Ibrahim, Y. E. (2018). "Seismic risk analysis of multistory reinforced concrete structures in Saudi Arabia." *Case Studies in Construction Materials,* 9, e00192.

[9] Vamvatsikos, D., and Cornell, C. A. (2002). "Incremental dynamic analysis." *Earthquake Engineering and Structural Dynamics,* 31(3), 491-514.

[10] Zhang, R., Chen, Z., Chen, S., Zheng, J., Buyukozturk, O., and Sun, H. (2019). "Deep long short-term memory networks for nonlinear structural seismic response prediction." *Computers and Structures,* 220, 55-68.

[11] Lavaei, A., and Lohrasbi, A. (2012). "Dynamic analysis of structures using neural networks." *In the Proceedings of 15th World Conference on Earthquake Engineering,* Lisbon, Portugal.

[12] Gidaris, I., Taflanidis, A. A., and Mavroeidis, G. P. (2015). "Kriging metamodeling in seismic risk assessment based on stochastic ground motion models." *Earthquake Engineering and Structural Dynamics,* 44, 2377-2399.

[13] Alexandridis, A. (2013). "Evolving RBF neural networks for adaptive soft-sensor design." *International Journal of Neural Systems,* 23(6), 1350029.

[14] Papadrakakis, M., and Lagaros, N. D. (2002). "Reliability-based structural optimization using neural networks and Monte Carlo simulation." *Computer Methods in Applied Mechanics and Engineering,* 191(32), 3491-3507.

[15] Lagaros, N. D., Plevris, V., and Papadrakakis, M. (2010). "Neurocomputing strategies for solving reliability-robust design optimization problems." *Engineering Computations,* 27(7), 819-840.

[16] Hurtado, J. E., and Alvarez, D. A. (2001). "Neural network-based reliability analysis: a comparative study." *Computer Methods in Applied Mechanics and Engineering,* 191(1-2), 113-132.

[17] Lagaros, N. D., and Fragiadakis, M. (2007). "Fragility assessment of steel frames using neural networks." *Earthquake Spectra,* 23(4), 735-752.

[18] Khandel, O., Soliman, M., Floyd, R. W., and Murray, C. D. (2020). "Performance assessment of prestressd concrete bridge girders using fiber optic sensors and artificial neural networks." *Structure and Infrastructure Engineering*.

[19] Ok, S., Son, W., and Lim, Y. M. (2012). "A study of the use of artificial neural networks to estimate dynamic displacements due to dynamic loads in bridges." *In the Proceedings of Journal of Physics: Conference Series, 382-012032,* University of Glasgow, Scotland.

[20] Masri, S. F., Nakamura, M., Chassiakos, A. G., and Caughey, T. K. (1996). "Neural network approach to detection of changes in structural parameters." *Journal of Engineering Mechanics,* 122(4), 350-360.

[21] Pal, S. K., and Mitra, S. (1992). "Multilayer perceptron, fuzzy sets, and classification." *In the Proceedings of IEEE Transactions on Neural Networks,* 3, 683-697.

[22] Patra, J. C., and Bornand, C. (2010). "Nonlinear dynamic system identification using Legendre neural network." *In the Proceedings of the International Joint Conference on Neural Networks,* Barcelona, Spain.

[23] Arjovsky, M., Shah, A., and Bengio, Y. (2016). "Unitary Evolution Recurrent Neural Networks." *In the Proceedings of the 33rd International Conference on Machine Learning,* New York City, New York, USA.

[24] Lin, T., Horne, B. G., Tino, P., and Giles, C. L. (1996). "Learning long-term dependencies in NARX recurrent neural networks." *IEEE Transaction on Neural Networks,* 7, 1329-1338.

[25] Wu, R-T., and Jahanshahi, M. R. (2018). "Deep convolutional neural network for structural dynamic response estimation and system identification." *Journal of Engineering Mechanics,* 145(1), 0401825.

[26] Ouyang, HT. (2017). "Nonlinear autoregressive neural networks with external inputs for forecasting of typhoon inundation level." *Environmental Monitoring and Assessment,* 189(8), 376.

[27] Ruiz, L. G. B., Cuellar. M. P., Calvo-Flores, M. D., and Jimenez, M. C. (2016). "An application of non-linear autoregressive neural networks to predict energy consumption in public buildings." *Energies,* 9(9), 684.

[28] Celik, O. C., and Ellingwood, B. R. (2009). "Seismic risk assessment of gravity load designed reinforced concrete frames subjected to mid-America ground motions." *Journal of Structural Engineering,* 135(4), 414-424.

[29] Ibarra L. F., and Krawinkler H. (2005). "Global collapse of frame structures under seismic excitations." *Blume Earthquake Engineering Center,* Technical Report No.152.

[30] Sabetta F., Goretti A., and Lucantoni A. (1998). "Empirical fragility curves from damage surveys and estimated strong ground motion." *In the Proceedings of the 11th European Conference on Earthquake Engineering,* Paris, France.

[31] Jaiswal, K. S., Aspinall W. P., Perkins D., and Porter, K. A. (2012). "Use of expert judgment elicitation to estimate seismic vulnerability of selected building types." *In the Proceedings of 15th World Conference on Earthquake Engineering,* Lisbon, Portugal.

[32] Sheikh, I. A., Khandel, O., Soliman, M., Haase, J. S., and Jaiswal, P. (2019). "An integrated framework for seismic risk assessment of reinforced concrete buildings based on structural health monitoring." *In the Proceedings of the IABSE,* New York City, New York, USA.

[33] Yi, J. H., Kim, D., Go, S., Kim, J. T., Park, J. H., Feng, M. Q., and Kang, K. S. (2012). "Application of structural health monitoring system for reliable seismic performance evaluation of infrastructures." *Advances in Structural Engineering,* 15(6), 955-967.

[34] Rainieri, C., Fabbrocino, G., and Cosenza, E. (2010). "Integrated seismic early warning and structural health monitoring of critical civil infrastructures in seismically prone areas." *Structural Health Monitoring,* 10(3), 291-308.

[35] CSI. (2018). "SAP2000 integrated software for structural analysis and design and reference manual." *Computers and Structure Inc.,* Berkely, California.

[36] Newmark, N. M. (1959). "A method of computation for structural dynamics." *Journal of Engineering Mechanics Division,* 85(3), 67-94.

[37] Hilber, H. M., Hughes, T. J., and Taylor, R. L. (1977). "Improved numerical dissipation for time integration algorithms in structural dynamics." *Earthquake Engineering and Structural Dynamics,* 5(3), 283-292.

[38] Lallemant, D., Kiremidjian, A., and Burton, H. (2015). "Statistical procedures for developing earthquake damage fragility curves." *Earthquake Engineering and Structural Dynamics,* 44(9), 1373-1389.

[39] Baker, J. W. (2015). "Efficient analytical fragility function fitting using dynamic structural analysis." *Earthquake Spectra,* 31(1), 579-599.

[40] Siegelmann, H. T., Horne, T., and Giles, C. L. (1997). "Computational capabilities of recurrent NARX neural networks." *IEEE Transactions on Systems, Man and Cybernetics,* 27(2), 208-215.

[41] Menezes Jr., J. M. P., and Barreto, G. A. (2006). "A new look at nonlinear time series prediction with NARX recurrent neural network." *In the Proceedings of the Ninth Brazilian Symposium on Neural Networks,* Ribeirao Preto, Brazil.

[42] Montana, D. J., and Davis, L. (1989). "Training feedforward neural networks using genetic algorithms." *In the Proceedings of the 11th International Joint Conference on Artificial Intelligence,* Michigan, USA.

[43] Sibi, P., Jones, S. A., and Siddarth, P. (2013). "Analysis of different activation functions using back propagation neural networks." *Journal of Theoretical and Applied Information Technology,* 47(3), 1264-1268.

[44] Wang, Z., Pedroni, N., Zentner, I., and Zio, E. (2018). "Seismic fragility analysis with artificial neural networks: Application to nuclear power plant equipment." *Engineering Structures,* 162, 213-225.

[45] Joghataie, A. and Farrokh, M. (2008). "Dynamic analysis of nonlinear frames by Prandtl neural networks." *Journal of Engineering Mechanics,* 134(11), 961-969.

[46] Mathworks. (2019). "MATLAB: The language of technical computing and user manual." Retrieved from https://www.mathworks.com.

[47] Mander, J. B., Priestley, M. J. N., and Park, R. (1988). "Theoretical stress-strain model for confined concrete." *Journal of Structural Engineering,* 114(8), 1804-1826.

[48] Salihovic, A., and Ademovic, N. (2017). "Nonlinear analysis of reinforced concrete frame under lateral load." *Coupled Systems Mechanics,* 6(4), 523-537.

[49] Celik, O. C., and Ellingwood, B. R. (2009). "Seismic risk assessment of gravity load designed reinforced concrete frames subjected to mid-America ground motions." *Journal of Structural Engineering,* 135(4), 414-424.

[50] PEER/ATC-72. (2010). "Modeling and acceptance criteria for seismic design and analysis of tall buildings." *Applied Technology Council,* Redwood, California.

[51] Federal Emergency Management Agency. (2000). "FEMA 356, Prestandard and commentary for the seismic rehabilitation of buildings." Washington DC.

[52] Takeda, T., Sozen, M. A., and Nielsen, N. N. (1970). "Reinforced concrete response to simulated earthquakes." *Journal of Structural Division,* 96(ST12), 2557-2573.

[53] Otani S. (1980). "Nonlinear dynamic analysis of reinforced concrete building structures." *Canadian Journal of Civil Engineering,* 7, 333-344.

[54] PEER. (2008). “Pacific Earthquake Engineering Research Center (NGA-West2).” Berkeley, California. Retrieved from https://peer.berkeley.edu/ngawest2.

[55] Joyner, W. B., and Boore, D. M. (1981). “Peak horizontal acceleration and velocity from strong motion records including records from the 1979 imperial valley, California earthquake.” *Seismological Society of America,* 71(6), 2011-2038.

[56] MacKay, D. (1992). “A practical Bayesian framework for backpropagation networks.” *Neural Computation,* 4(3), 448.

VITA

Imran Ahmed Sheikh

Candidate for the Degree of

Master of Science

Thesis: APPLICATION OF NONLINEAR AUTOREGRESSIVE NEURAL NETWORKS WITH EXOGENOUS INPUTS (NARX) IN SEISMIC FRAGILITY ANALYSIS OF BUILDINGS

Major Field: Civil Engineering

Biographical:

Education:

Completed the requirements for the Master of Science in Civil Engineering at Oklahoma State University, Stillwater, Oklahoma in July, 2020.

Completed the requirements for the Bachelor of Science in Civil Engineering at National University of Sciences and Technology, Islamabad, Pakistan in 2015.